NJC

RSC Publishing

PAPER

View Article Online
View Journal | View Issue

Cite this: *New J. Chem.*, 2013, **37**, 1554

Molecular binding behaviors of triazole-bridged bis(β-cyclodextrin)s towards cinchona alkaloids†

Ying-Ming Zhang, Hong-Zhong Chen, Yong Chen, Fei Ding and Yu Liu*

Received (in Montpellier, France) 19th February 2013,
Accepted 27th February 2013

DOI: 10.1039/c3nj00193h

www.rsc.org/njc

Three bridged bis(β-cyclodextrin)s **3–5** possessing 1,2,3-triazole moieties and polyether chains of different lengths have been synthesized by click reactions in high yields. Their binding affinities towards four cinchona alkaloids, namely, cinchonine, cinchonidine, quinine, and quinidine, have been quantitatively investigated by means of spectrophotometric titrations and 2D NMR spectroscopy. Spectroscopic analyses demonstrated that, compared with native β- and γ-cyclodextrins, bridged bis(β-cyclodextrin)s with a rigid spacer give enhanced molecular binding abilities towards the selected substrates. Moreover, the factors resulting in the significant differences in photophysical behaviors of bridged bis(β-cyclodextrin)s towards cinchona alkaloids are discussed from the viewpoint of the binding geometry of host–guest complexes, revealing that the aromatic ring containing the nitrogen atom of quinine is accommodated in the cavity of **3**, whereas the rings of cinchonine, cinchonidine, and quinidine are located out of the cavity of the cyclodextrin and are exposed to aqueous media.

1. Introduction

Cooperativity is ubiquitously encountered in diverse biological processes,[1] including DNA double-stranded helicates, peptide–polysaccharide interactions, as well as dioxygen binding and transport to hemoglobin, in which the initial binding of a substrate to one subunit of a receptor may influence the complexation ability or catalytic activity towards a subsequent binding event, thus remarkably maximizing the substrate affinity and selectivity with a nonlinear dependence. With respect to the cooperative effect in the artificial systems, supramolecular positive cooperativity in host–guest ensembles has emerged to be an effective strategy to integrate the constitutive building blocks into multidimensional nanodevices. Through a perfect alignment of multipoint binding sites, one can precisely control the intermolecular interactions in the spontaneous formation of self-assemblies, and the physicochemical functionalities could be more dramatically enhanced than that of its corresponding individual counterpart. Among the numerous synthetic receptors, cyclodextrin (CD) and its derivatives for molecular recognition have attracted an upsurge of interest in exploring and mimicking natural cooperative binding systems with high efficiency and selectivity. In that framework, bridged CD dimers, possessing two binding sites in close proximity, exhibit enhanced binding abilities towards guest molecules, compared with native and mono-modified CDs.[2] Therefore, considerable efforts have been devoted in this field of supramolecular chemistry to designing and synthesizing various CD dimers with considerable structural diversity to achieve the cooperative binding processes. For instance, Vargas-Berenguel and coworkers studied the supramolecular behavior between ferrocene-β-CD conjugates and bile salts, revealing the controlled redox-sensing abilities and guest-induced conformational changes upon complexation.[3] The complexation of some bridged CD dimers linked by rigid tethers with bile salts was also reported by the same group.[4] Mao *et al.* reported several divalent transitional metal-based complexes bearing two hydrophobic CD domains, exhibiting a high acceleration in the catalytic hydrolysis of carboxylic acid esters and phosphate esters.[5] We also investigated the molecular recognition processes of some bridged and metallobridged bis(β-CD)s containing functional tethers towards a series of bile salts, organic dyes, nucleic acid bases, oligopeptides, drug molecules, porphyrins, and volatile compounds in the past few decades,[2b,6] showing satisfactory molecular selectivity and enhanced binding abilities in these supramolecular nanoarchitectures.

Inspired by our ongoing interest in supramolecular cooperativity related to molecular recognition and binding thermodynamics, in the present work, we synthesized three novel bridged bis(β-CD)s linked by different lengths of tether to further elucidate the detailed

Department of Chemistry, State Key Laboratory of Elemento-Organic Chemistry, Nankai University, Tianjin 300071, People's Republic of China.
E-mail: yuliu@nankai.edu.cn

† Electronic supplementary information (ESI) available: Characterization data for compounds **3–5**, fluorescence spectral changes of **3**/CIN and **4**/QUN systems, comparative photophysical properties, complex stability constants, and structural information of host–guest complexes, as well as 2D ROESY spectrum of **3**/CID system. See DOI: 10.1039/c3nj00193h

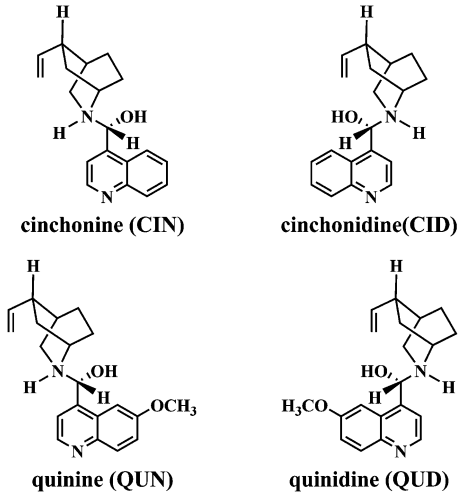

Chart 1 Structures of employed guest molecules

recognition mechanism of bridged bis(β-CD)s towards substrates. Moreover, two pairs of the most commercial and important anti-malarial drugs with different chiral positions,[7] *i.e.* cinchonine (CIN), cinchonidine (CID), quinine (QUN), and quinidine (QUD), were chosen to comprehensively study the significance of cooperative noncovalent interactions between dimeric hosts and model guests (Chart 1). Molecular recognition and binding geometries towards guest molecules were evaluated by spectrophotometric titrations and 2D NMR experiments in aqueous solution. These studies will help us gain a deeper insight into the molecular recognition mechanism of cinchona alkaloids with CD dimers and consequently improve their further application in drug carriers and enantiomeric discrimination.

2. Results and discussion

2.1 Synthesis of host compounds

The synthetic routes of compound **3–5** are described in Scheme 1. The terminal dialkynyl derivatives were prepared by the reaction of ethylene glycol with propargyl bromide according to the reported literature.[8] Then, triazole-linked bis(β-CD)s **3–5** were synthesized by a 'click chemistry' reaction with mono-6-deoxyl-6-azido-β-CD[9] in DMF–H_2O mixture. Benefiting from the good solubilization ability of β-CD units, hosts **3–5** showed satisfactory solubilities up to 0.02 M in water. The compositions of all products were comprehensively verified by NMR spectroscopy, ESI-MS, and elemental analysis (Fig. S1–S9 in ESI†).

2.2 Spectroscopic titrations

For the quantitative assessment of inclusion complexation behaviors of hosts and guests, spectroscopic titration experiments were performed in phosphate buffer solution to determine the complex stability constant (K_S) and Gibbs free-energy change (ΔG°) of hosts **3–5** with CIN, CID, QUN, and QUD. Considering that cinchona alkaloids could be simultaneously encapsulated with two β- or γ-CDs to form stable sandwich-type supramolecular complexes,[10] the inclusion equilibrium of host (H) with guest (G) is expressed by eqn (1), where K_S represents the complex formation constant:

$$H + G \overset{K_S}{\rightleftharpoons} HG \quad (1)$$

In our fluorescence titration experiments, the guest concentration was fixed, and its relative fluorescence intensity was accordingly changed upon the addition of host compound. It is assumed that the changes in fluorescence intensity should be proportional to the concentration of host–guest complex in solution. Therefore, using a nonlinear least-squares curve-fitting method in eqn (2),[11] we can obtain the complex stability constant (K_S) by analyzing sequential changes in fluorescence intensity (ΔI_f) at varying concentrations of CDs.

$$\Delta I_f = \frac{\alpha\left([H]_0 + [G]_0 + 1/K_S\right) \pm \sqrt{\alpha^2\left([H]_0 + [G]_0 + 1/K_S\right)^2 - 4\alpha^2[H]_0[G]_0}}{2} \quad (2)$$

where α, $[H]_0$, and $[G]_0$ refer to the proportionality coefficient, and total concentrations of host and cinchona alkaloid molecules, respectively. Moreover, according to eqn (3), the knowledge of the complex stability constant (K_S) enables the calculation of standard free energy (ΔG°):

$$\Delta G^\circ = -RT \ln K_S \quad (3)$$

where R is the gas constant and T is the absolute temperature.

Possessing a quinoline ring as the chromophoric group, cinchona alkaloids are strongly fluorescent in water, and their photophysical properties are very sensitive to the hydrophobic microenvironment, which enables us to consider them as spectral probes to investigate the inclusion complexation with hosts **3–5**.[12] The comparative photophysical properties of hosts **3–5** with cinchona alkaloids are listed in Table S1 (ESI†). The typical curve fitting plots of CID and CIN in an excess amount of **3** are illustrated in Fig. 1 and Fig. S10 (ESI†), giving good fits between experimental and calculated data for 1 : 1 complexation stoichiometry in our system. The fluorescence intensity of CID and CIN was dramatically enhanced by 20 times in the presence of host **3**. Therefore, the binding constants (K_S) of **3**/CIN and **3**/CID systems can be calculated as 4.04×10^2 and 3.88×10^2 M^{-1}, respectively, by a nonlinear least-squares curve-fitting method as elucidated above (Fig. 1 and Fig. S10, ESI,† inset).

In contrast, as discerned in Fig. 2, approximately 40% of the fluorescence intensity of QUN gradually decreased with the stepwise addition of host **3**, which was strikingly distinctive from the **3**/QUD system with an enhancement in fluorescence intensity and a large bathochromic shift of emission peak from 382 nm to 393 nm (Fig. 3). Moreover, employed the similar fluorescence titration method, the K_S values of **3** with QUN and QUD were determined to be 1.55×10^2 and 7.77×10^2 M^{-1}, respectively, corresponding to a diastereoisomer selectivity of *ca.* 1 : 5 (Fig. 2 and 3, inset). These interesting and infrequent photophysical behaviors may indicate the different binding

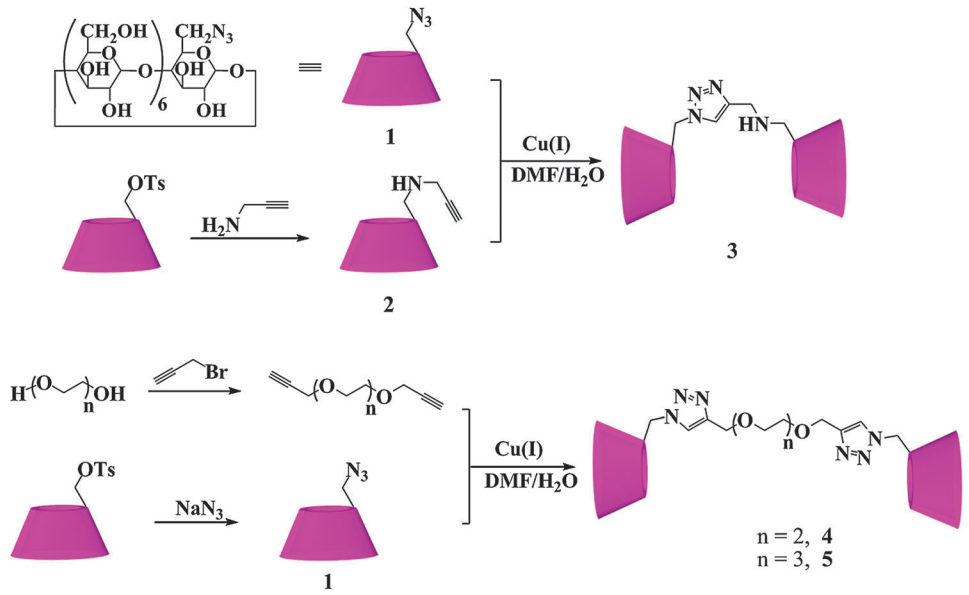

Scheme 1 Syntheses of host compounds **1–5**.

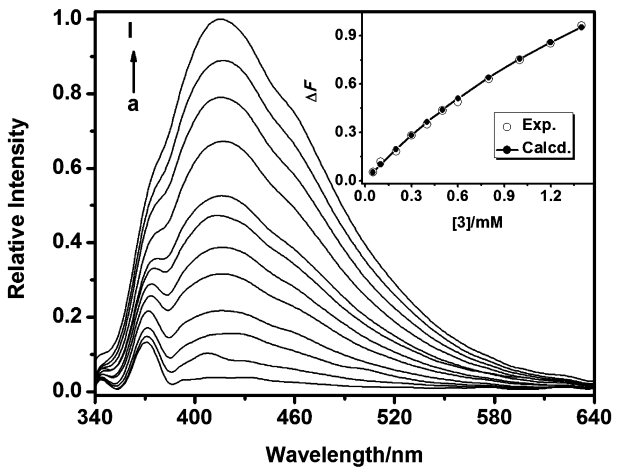

Fig. 1 Emission spectral changes of CID upon addition of **3** in phosphate buffer solution (0.1 M, pH 7.2) at 25 °C ([CID] = 7.2 × 10^{-6} M, [**3**] = 0, 0.05, 0.1, 0.2, 0.3, 0.4, 0.5, 0.6, 0.8, 1.0, 1.2, 1.4 × 10^{-3} M, respectively, from a to l). Inset: The nonlinear least squares analysis of the differential spectral changes (Δ*F*) at 415 nm to calculate the stability constant (K_S) between **3** and CID (λ_{ex} = 330 nm).

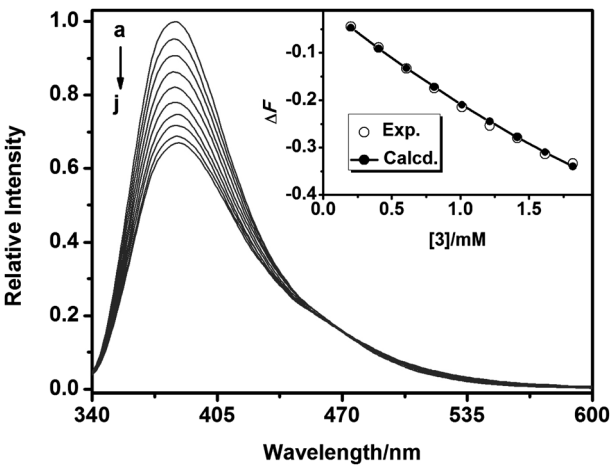

Fig. 2 Emission spectral changes of QUN upon addition of **3** in phosphate buffer solution (0.1 M, pH 7.2) at 25 °C ([QUN] = 1.0 × 10^{-5} M, [**3**] = 0, 0.2, 0.4, 0.6, 0.8, 1.0, 1.2, 1.4, 1.6, 1.8 × 10^{-3} M, respectively, from a to j). Inset: The nonlinear least squares analysis of the differential spectral changes (Δ*F*) at 380 nm to calculate the stability constant (K_S) between **3** and QUN (λ_{ex} = 330 nm).

modes in **3**/QUD and **3**/QUN complexes, which were further confirmed by 2D NMR experiments, as described below.

Subsequently, K_S and ΔG° values for each host–guest complex were obtained and summarized in Table 1. For a comparative purpose, these parameters for native β- and γ-CD with cinchona alkaloids in reported literature were also listed in Table 1. From Table 1, we can see that K_S values of dimeric β-CDs **3** with guest molecules are comparable to, or obviously larger than, those of native and monomeric CDs, whereas the dimeric β-CDs **5** with more flexible linker gave no reliable K_S values toward all the selected guests. For example, the binding constant of bis(β-CD) **3** with CID is 3.3 times higher than that of native β-CD, and the one with CIN is 3.7 times higher than that of native β-CD. Furthermore, in comparison to triazole-linked bis(β-CD) **3**, hosts **4** and **5** result in a much weaker affinity towards most guest molecules, decreasing with the following order: **3** > **4** > **5**. Surprisingly, it is noteworthy that the K_S value for the **4**/QUN complex was determined to be 5.52 × 10^2 M^{-1} (Fig. S11 in ESI†), which is ascribable to a better size–shape fitting efficiency between receptor and substrate. Obviously, bridged bis(β-CD)s can simultaneously afford two hydrophobic binding sites in close proximity, which jointly contribute to the effect of supramolecular positive cooperativity upon inclusion complexation, ultimately resulting in a significant enhancement in the original binding abilities of parent monomeric CDs.

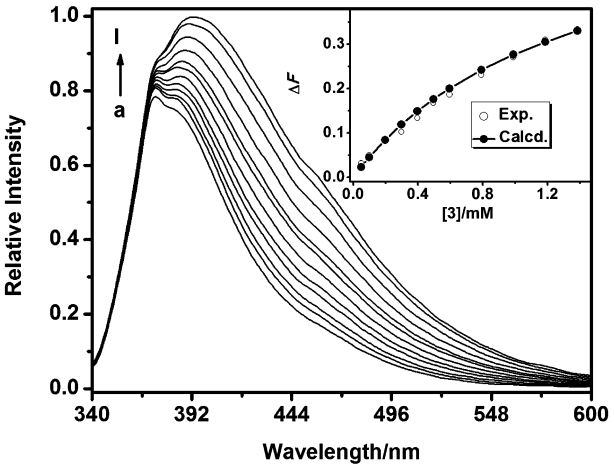

Fig. 3 Emission spectral changes of QUD upon addition of **3** in phosphate buffer solution (0.1 M, pH 7.2) at 25 °C ([QUD] = 1.0×10^{-5} M, [**3**] = 0, 0.05, 0.1, 0.2, 0.3, 0.4, 0.5, 0.6, 0.8, 1.0, 1.2, 1.4×10^{-3} M, respectively, from a to l). Inset: The nonlinear least squares analysis of the differential spectral changes (ΔF) at 395 nm to calculate the stability constant (K_S) between **3** and QUD (λ_{ex} = 330 nm).

Table 1 Complex stability constants (K_S M^{-1}) and Gibbs free-energy changes (ΔG°/kJ mol^{-1}) for the 1 : 1 inclusion complexes between cinchona alkaloids and native β-, γ-CD, and hosts **3–5** in phosphate buffer solution at 25 °C

Host	Guest	K_S	log K_S	ΔG°	Ref.
β-CD	CID	117	2.07	−11.8	*a*
	CIN	108	2.03	−11.6	*a*
	QUD	Not observed	—	—	*a*
	QUN	Not observed	—	—	*a*
γ-CD	CID	321	2.51	−14.3	*a*
	CIN	462	2.66	−15.2	*a*
	QUD	206	2.31	−13.2	*a*
	QUN	221	2.34	−13.4	*a*
3	CID	388	2.59	−14.8	*b*
	CIN	404	2.61	−14.9	*b*
	QUD	777	2.89	−16.5	*b*
	QUN	155	2.19	−12.5	*b*
4	CID	72	1.86	−10.6	*b*
	CIN	Not observed	—	—	*b*
	QUD	99	2.00	−11.4	*b*
	QUN	552	2.74	−15.6	*b*
5	CID	Not observed	—	—	*b*
	CIN	Not observed	—	—	*b*
	QUD	Not observed	—	—	*b*
	QUN	Not observed	—	—	*b*

— These K_S values (less than 10 M^{-1}) are very small and therefore cannot be accurately calculated. [a] Ref. 13. [b] This work.

Particularly, in comparison to **4** and **5** with a flexible polyether chain, the free movement of two adjacent cavities in bridged bis(β-CD) **3** is constrained to a large extent by a rigid linker with only one triazole moiety, and the conformational fixation of two cavities is quite appropriate to achieve a better binding ability by tightly encapsulating substrates as a pair of molecular tweezers.

To clarify the molecular selectivity between hosts and cinchona alkaloids, the changing profiles of complex stability constants were plotted in Fig. S12 (ESI†). It has been previously demonstrated that the binding abilities upon complexation of native β- and γ-CDs towards cinchona alkaloids are entirely different, in which CIN and CID are only partially included in the β-CD's cavity to show a relatively weak size-fit efficiency compared with γ-CD.[13] In contrast, benefiting from the cooperative binding of dimeric CDs, the K_S values of resulting complexes of host **3** with CID and CIN are much higher than that of native β-CD. In the case of complex **4**/QUN, the length and flexibility of polyether chains, as well as the synergistic actions of two adjacent CD's cavities, emerge to be the predominant forces to trap the chiral substrate in the molecular recognition process ($K_S^{4/QUN}/K_S^{3/QUN}$ = 3.6). Moreover, along with the increase of spacer length from diethylene glycol to triethylene glycol, the indefinite location extremely overwhelms their cooperativity arising from two neighboring CDs, leading to the poor binding behavior in host **5**.

2.3 Binding mode

2D NMR spectroscopy has become a powerful tool to obtain the structural information about the orientation of substituent or accommodated guest molecule by measuring intermolecular dipolar cross-correlations.[14] It is generally accepted that, if two protons are located in spatial proximity, a clear nuclear Overhauser enhancement (NOE) cross-correlation should be observed between protons of the guest molecule and interior protons of the CD cavity (H3, H5, and H6). According to the relative intensity of these NOE cross-peaks, one may estimate the binding mode between CD derivatives and guest molecules. On this basis, rotating-frame Overhauser effect spectroscopy (ROESY) experiments were employed to investigate the inclusion geometry of bis(β-CD) **3** with cinchona alkaloids in D_2O at 25 °C.

As discerned from Fig. S13 (ESI†), NOE correlations between protons of the aliphatic ring of CID and H5 protons of β-CD (peaks A and B), as well as those between protons of the ethenyl group of CID and H5 protons of β-CD (peaks C and D) jointly demonstrate that the 3-ethenyl-1-azabicyclo[2.2.2]octane moiety of CID was deeply accommodated in the cavity of β-CD from the primary face. Similarly, in the case of the **3**/CIN system, besides NOE correlations between protons of the aliphatic and ethenyl moiety of CIN and H5 protons of β-CD (peaks B and C in Fig. 4), it can be found that the phenyl ring of CIN was also shallowly included in the cavity of another β-CD (peak A in Fig. 4).

Comparatively, NOE cross-peaks between protons of the aromatic ring of QUN and H5 protons of **3** (peaks E and F in Fig. 5) were clearly observed in the ROESY spectrum, implying that the quinoline ring was deeply included in the β-CD cavity. Moreover, NOE correlations between protons of the ethenyl moiety of QUN and H5/H6 protons of **3** (peaks C and D), as well as those between protons of the aliphatic ring of QUN and interior protons of **3** (peaks A and B) indicate that the 3-ethenyl-1-azabicyclo[2.2.2]octane moiety of QUN was concurrently located in the hydrophobic cavity of β-CD. Conversely, the ROESY spectrum of the **3**/QUD system in Fig. 6 showed NOE correlations of the aliphatic ring and ethenyl group of QUD with H5 protons of β-CD in **3** (peaks B and C), distinctly indicating that the nonaromatic ring of QUD was included at the primary face of β-CD. Moreover, no obvious NOE correlation was observed between the protons of β-CD and the quinoline ring of QUD in the aromatic region, except the weak NOE

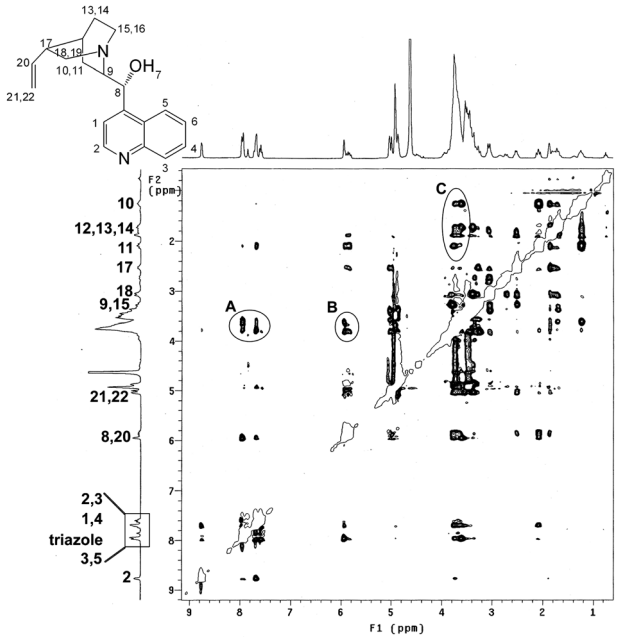

Fig. 4 ^{1}H ROESY spectrum of the **3**/CIN system with a mixing time of 0.25 s (300 MHz, D_2O, 25 °C).

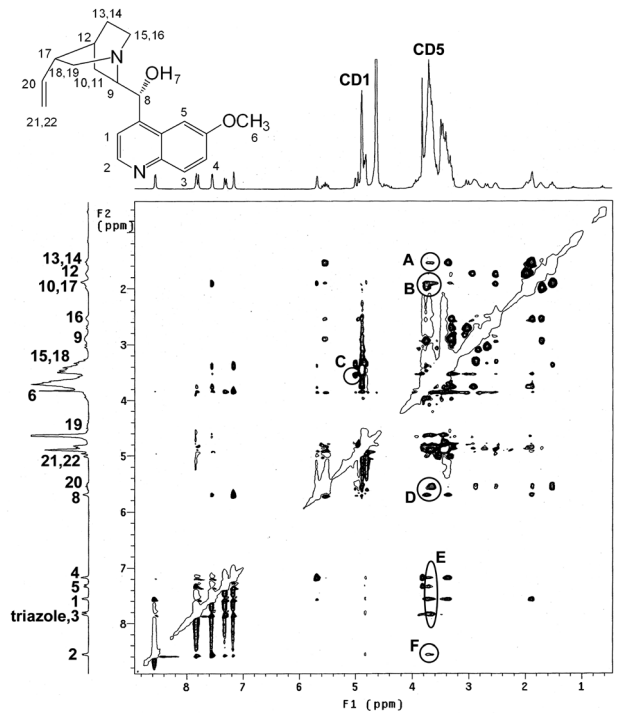

Fig. 5 ^{1}H ROESY spectrum of complex **3** and QUN after a mixing time of 0.24 s (300 MHz, D_2O, 25 °C).

correlations between the pyridyl moiety and CD's cavity (peak A). In comparison to the 3/QUD system, it is reasonable to conclude a deeper penetration of QUN into the β-CD cavity of **3**. Therefore, based on 2D NMR results, the possible binding modes of **3** with cinchona alkaloids are shown in Fig. 7. The structural information of host–guest complexation between

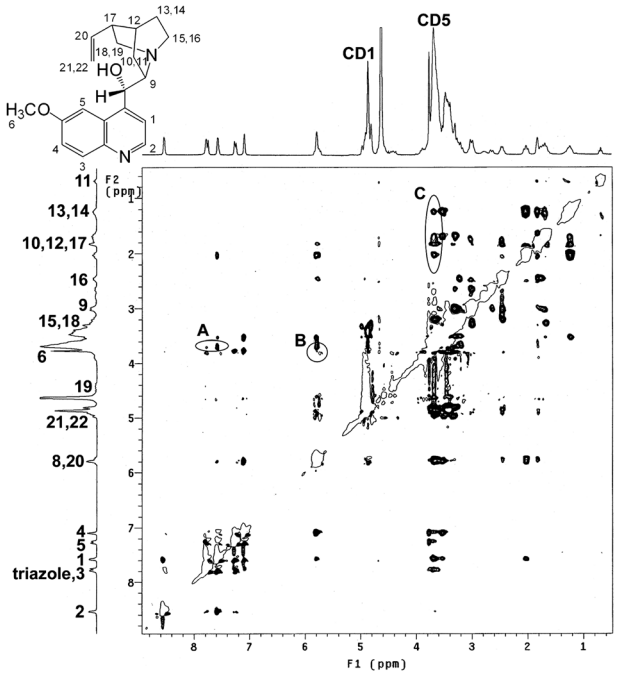

Fig. 6 ^{1}H ROESY spectrum of the **3**/QUD system with a mixing time of 0.25 s (300 MHz, D_2O, 25 °C).

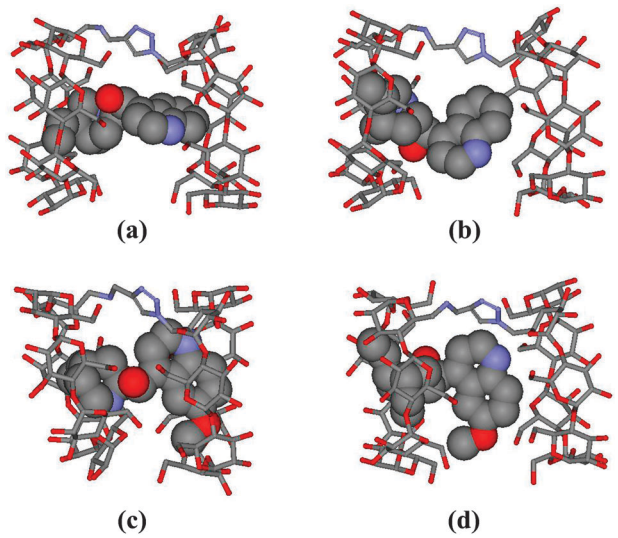

Fig. 7 Plausible molecular structures and molecular modeling of (a) **3**/CIN, (b) **3**/CID, (c) **3**/QUN, and (d) **3**/QUD inclusion complexes.

cinchona alkaloids and hosts **3** is summarized in Table S2 (ESI†).

These conformational differences in 2D NMR data give more detailed information of the noncovalent interaction of bridged bis(β-CD)s with guests and reinforce the aforementioned photophysical behaviors in fluorescence spectroscopic analyses. The driving force for complexation of CIN and CID with bridged bis(β-CD)s involves no direct interaction of the nitrogen heteroatom with the cavity of β-CD. The hydrophobic nature of the cyclodextrin cavity could offer a microenvironment to decrease

the random collision of free guests and prevent them from interacting with solvent molecules, subsequently leading to the enhancement of fluorescence intensity in **3**/CIN and **3**/CID systems. However, for the **3**/QUN complex, since the aromatic ring containing the nitrogen atom was deeply embedded in the β-CD cavity, specific inductive effects of the nitrogen heteroatom with the higher electron density of glycosidic oxygens in β-CD could deactivate guest molecules and then result in the fluorescence quenching in solution,[15] as exemplified by the quenching of acridine in the presence of β-CD.[16] Additionally, the non-covalent interactions in host–guest complexation play crucial roles to greatly facilitate the lone electron pairs of the nitrogen atom of the 1,2,3-triazole moiety close to the quinoline fluorophore, which results in an intermolecular photo-induced electron transfer *via* a nonradiative pathway to quench the fluorescence of the **3**/QUN complex.[17]

3. Conclusions

In conclusion, three triazole-linked bridged bis(β-CD)s **3–5** were newly synthesized, and their cooperative binding behaviors with four cinchona alkaloids were systemically investigated in aqueous media under neutral conditions. The length and flexibility of linkers in host molecules and guest chirality can profoundly affect binding abilities and thus lead to the contrasting binding geometry and photophysical behaviors towards substrates. Generally, the complex stability constants steadily decrease with increasing the length and flexibility of tethered moieties in our system. As a consequence, the dimeric host **3** linked by a short and rigid polyether chain presents the strongest binding affinities for most of the cinchona alkaloids in terms of the good size-fit relationship and a joint contribution of noncovalent bonding interactions (*i.e.* $K_S^{3/CID}/K_S^{\beta\text{-}CD/CID}$ = 3.3 and $K_S^{3/CIN}/K_S^{\beta\text{-}CD/CIN}$ = 3.7). Moreover, it is interesting to note that host **4** gives good recognition ability for QUD/QUN pair ($K_S^{4/QUN}/K_S^{4/QUD}$ = 5.6), originating from rational arrangement to achieve a spatially controllable complex. The structure-dependent complexation in this work emphasizes that utilization of size/shape matching in conjunction with other supramolecular noncovalent forces relative to the host–guest distance and contact surface area, such as van der Waals and hydrophobic interactions, is highly desirable for an effective binding process in aqueous media. The obtained results will pave a practical way to deeply understand the thermodynamics–structure relationship and the supramolecular positive cooperativity in many living systems.

4. Experimental section

4.1 Instrumentation

NMR spectra were recorded on a 300 or 400 MHz spectrometer. Mass spectra were performed on an ESI mode MS. Elemental analyses were measured by a conventional element analyzer. The plausible modeling structure was optimized by the molecular mechanics method with Dreiding forcefield. Fluorescence spectra were measured in a conventional quartz cell (10 × 10 × 45 mm) on a spectrometer employing the single photon counting technique with a temperature controller. The excitation wavelength for all four cinchona alkaloids was 330 nm. The stepwise addition of a known concentration of hosts to a solution of cinchona alkaloid causes significant changes in the fluorescence intensity of guests. According to fluorescence spectral changes of guest molecules, the complex stability constant (K_S) upon addition of host molecules could be calculated by the nonlinear least-squares analysis.

4.2 Materials

All chemicals were used as reagent grade without further purification unless noted. Cinchona alkaloids were purchased from commercial resources. Reagent grade β-CD was recrystallized twice from water and dried *in vacuo* at 80 °C for 24 h prior to use. The terminal dialkynyl derivatives[8] of 4,7,10-trioxahexadeca-1,12-diyne and 4,7,10,13-tetraoxahexadeca-1,15-diyne, mono-6-deoxyl-6-azido-β-CD,[9] and propargylamine modified β-cyclodextrin (**2**)[18] were prepared according to the reported methods. The phosphate buffer solution of pH 7.2 in spectroscopic titrations was prepared by dissolving 25.79 g $Na_2HPO_4{\cdot}12H_2O$ and 4.36 g $NaH_2PO_4{\cdot}2H_2O$ in 1.0 L distilled and deionized water to make a 0.1 M solution.

4.3 Synthesis of triazole-bridged bis(β-CD) (3)

A solution of mono-6-deoxyl-6-azido-β-CD (464 mg, 0.4 mmol) in 10 mL of water was added to a solution of compound **2** (469 mg, 0.4 mmol) and $CuSO_4{\cdot}5H_2O$ (200 mg, 0.8 mmol) in 20 mL of water. The mixture was heated at 70 °C for 10 min, and then sodium ascorbate (400 mg, 2.0 mmol) in water (10 mL) was added. The resulting mixture was kept at 70 °C under an atmosphere of nitrogen for 24 h. Insoluble precipitates were removed by filtration, and the crude product was subjected to a medium-pressure liquid chromatography (MPLC) system using a gradient elution system of distilled water and ethanol gradient with ethanol from 0 to 9% at a flow rate of 5 mL min^{-1}. The detector wavelength was set at 245 nm. After drying under vacuum, the target compound was obtained as a light brown solid in 50% yield. ^{1}H NMR (400 MHz, D_2O, ppm): δ 7.75 (s, 1H), 4.78–4.95 (m, 14H), 3.19–4.00 (m, 82H), 2.95–2.98 (m, 1H), 2.85–2.88 (m, 1H), 2.61–2.63 (m, 2H); ^{13}C NMR (100 MHz, DMSO-d_6, ppm): δ 146.0, 124.1, 101.9, 101.5, 83.3, 81.5, 73.0, 72.7, 72.4, 72.2, 72.0, 71.6, 59.9, 59.1, 50.1, 48.9, 44.5. Anal. calcd for $C_{87}H_{142}N_4O_{68}{\cdot}15H_2O$: C, 40.00; H, 6.19; N, 2.49. Found: C, 40.16; H, 6.66; N, 2.15. MALDI-MS *m*/*z*: 2353.77 $[M + Na]^+$.

4.4 Synthesis of triazole-bridged bis(β-CD) (4)

A solution of mono-6-deoxyl-6-azido-β-CD (1.3 g, 1.1 mmol) and $CuSO_4{\cdot}5H_2O$ (400 mg, 1.6 mmol) in 15 mL of water was added to a solution of 4,7,10-trioxahexadeca-1,12-diyne (80 mg, 0.44 mmol) in 20 mL of DMF. The mixture was heated at 70 °C for 10 min, and then sodium ascorbate (800 mg, 4.0 mmol) in water (10 mL) was added. The resulting mixture was kept at 70 °C under an atmosphere of nitrogen for 24 h. Insoluble precipitates were removed by filtration, and the crude product was subjected to a medium-pressure liquid chromatography (MPLC) system using a gradient elution system of distilled

water and ethanol gradient with ethanol from 0 to 12% at a flow rate of 8 mL min^{-1}. The detector wavelength was set at 245 nm. After drying under vacuum, the target compound was obtained as a light yellow solid in 65% yield. ^{1}H NMR (400 MHz, D_2O, ppm): δ 7.67–7.98 (m, 2H), 4.88–5.10 (m, 14H), 4.45–4.62 (m, 4H), 3.37–4.15 (m, 88H), 3.06–3.09 (m, 2H), 2.72–2.74 (m, 2H); ^{13}C NMR (100 MHz, DMSO-d_6, ppm): δ 143.7, 124.9, 102.2, 102.0, 101.9, 101.2, 83.4, 82.0, 81.4, 80.9, 72.3, 72.0, 68.9, 63.3, 60.1, 59.9, 58.9, 50.2. Anal. calcd for $C_{94}H_{152}N_6O_{71}\cdot16H_2O$: C, 40.46; H, 6.65; N, 3.01. Found: C, 40.34; H, 6.50; N, 3.23. MALDI-MS *m/z*: 2524.84 $[M + Na]^+$, 2538.82 $[M + K]^+$.

4.5 Synthesis of triazole-bridged bis(β-CD) (5)

The host compound **5** was prepared by the same procedure as described above using 4,7,10,13-tetraoxahexadeca-1,15-diyne as starting material in 70% yield. ^{1}H NMR (400 MHz, D_2O, ppm): δ 7.82–8.01 (m, 2H), 4.91–5.13 (m, 14H), 4.57–4.65 (m, 4H), 3.35–4.18 (m, 92H), 3.09–3.12 (m, 2H), 2.75–2.78 (m, 2H); ^{13}C NMR (100 MHz, DMSO-d_6, ppm): δ 1 143.7, 124.9, 102.2, 102.0, 101.9, 101.2, 83.4, 82.0, 81.4, 80.9, 73.0, 72.6, 72.3, 72.0, 71.7, 69.9, 69.7, 69.6, 68.9, 63.3, 59.9, 58.9, 50.3. Anal. calcd for $C_{96}H_{156}N_6O_{72}\cdot18H_2O$: C, 40.17; H, 6.74; N, 2.93. Found: C, 49.87; H, 6.81; N, 3.01. MALDI-MS *m/z*: 2568.86 $[M + Na]^+$, 2583.85 $[M + K]^+$.

Acknowledgements

This work is financially supported by 973 Program (2011CB932502), NNSFC (No. 20932004 and 21102075), the Fundamental Research Funds for the Central Universities, and the Specialized Research Fund for the Doctoral Program of Higher Education (20110031120014).

Notes and references

1 (*a*) S. Shinkai, M. Ikeda, A. Sugasaki and M. Takeuchi, *Acc. Chem. Res.*, 2001, **34**, 494–503; (*b*) D. H. Williams, E. Stephens, D. P. O'Brien and M. Zhou, *Angew. Chem., Int. Ed.*, 2004, **43**, 6596–6616; (*c*) J. D. Badjić, A. Nelson, S. J. Cantrill, W. B. Turnbull and J. F. Stoddart, *Acc. Chem. Res.*, 2005, **38**, 723–732; (*d*) E. M. Pérez and N. Martín, *Chem. Soc. Rev.*, 2008, **37**, 1512–1519; (*e*) Y. Hua and A. H. Flood, *Chem. Soc. Rev.*, 2010, **39**, 1262–1271; (*f*) Y. Chen, Y.-M. Zhang and Y. Liu, *Isr. J. Chem.*, 2011, **51**, 515–524; (*g*) C. Wang, Z. Wang and X. Zhang, *Acc. Chem. Res.*, 2012, **45**, 608–618.

2 (*a*) R. Breslow and S. D. Dong, *Chem. Rev.*, 1998, **98**, 1997–2011; (*b*) A. Mulder, J. Huskens and D. N. Reinhoudt, *Org. Biomol. Chem.*, 2004, **2**, 3409–3424; (*c*) Y. Liu and Y. Chen, *Acc. Chem. Res.*, 2006, **39**, 681–691; (*d*) G. Wenz, B.-H. Han and A. Müller, *Chem. Rev.*, 2006, **106**, 782–817; (*e*) T. Ogoshi and A. Harada, *Sensors*, 2008, **8**, 4961–4982; (*f*) A. Aljarilla, J. C. López and J. Plumet, *Eur. J. Org. Chem.*, 2010, 6123–6143; (*g*) S. H. Choi and K. E. Geckeler, *J. Inclusion Phenom. Macrocyclic Chem.*, 2007, **57**, 257–260; (*h*) Y. Zhao, Y. C. Yang, H. Shi, H. Y. Zhu, R. Huang, C. M. Chi and Y. Zhao, *Helv. Chim. Acta*, 2010, **93**, 1136–1148.

3 J. M. Casas-Solvas, E. Ortiz-Salmerón, I. Fernández, L. García-Fuentes, F. Santoyo-González and A. Vargas-Berenguel, *Chem.–Eur. J.*, 2009, **15**, 8146–8162.

4 (*a*) J. M. Casas-Solvas, I. Quesada-Soriano, D. Carreño-Gázquez, J. J. Giménez-Martínez, L. García-Fuentes and A. Vargas-Berenguel, *Langmuir*, 2011, **27**, 9729–9737; (*b*) M. C. Martos-Maldonado, I. Quesada-Soriano, J. M. Casas-Solvas, L. García-Fuentes and A. Vargas-Berengu, *Eur. J. Org. Chem.*, 2012, 2560–2571.

5 (*a*) Y.-H. Zhou, M. Zhao, Z.-W. Mao and L.-N. Ji, *Chem.–Eur. J.*, 2008, **14**, 7193–7201; (*b*) S.-P. Tang, Y.-H. Zhou, H.-Y. Chen, C.-Y. Zhao, Z.-W. Mao and L.-N. Ji, *Chem.–Asian J.*, 2009, **4**, 1354–1360; (*c*) M. Zhao, H.-L. Wang, L. Zhang, C. Zhao, L.-N. Ji and Z.-W. Mao, *Chem. Commun.*, 2011, **47**, 7344–7346.

6 (*a*) Y. Chen, F. Li, B.-W. Liu, B.-P. Jiang, H.-Y. Zhang, L.-H. Wang and Y. Liu, *J. Phys. Chem. B*, 2010, **114**, 16147–16155; (*b*) B.-P. Jiang, D.-S. Guo and Y. Liu, *J. Org. Chem.*, 2010, **75**, 7258–7264; (*c*) L. Li, C.-F. Ke, H.-Y. Zhang and Y. Liu, *J. Org. Chem.*, 2010, **75**, 6673–6676; (*d*) Y.-M. Zhang, Y. Chen, R.-J. Zhuang and Y. Liu, *Photochem. Photobiol. Sci.*, 2011, **10**, 1393–1398.

7 (*a*) W. M. Braje, R. Wartchow and H. M. R Hoffmann, *Angew. Chem., Int. Ed.*, 1999, **38**, 2539–2543; (*b*) H. M. R. Hoffmann and J. Frackenpohl, *Eur. J. Org. Chem.*, 2004, 4293–4312.

8 S. André, M. Lahmann, H.-J. Gabius and S. Oscarson, *Mol. Pharmaceutics*, 2010, **7**, 2270–2279.

9 C. Hocquelet, J. Blu, C. K. Jankowski, S. Arseneau, D. Buisson and L. Mauclaire, *Tetrahedron*, 2006, **62**, 11963–11971.

10 X. Wen, Z. Liu, T. Zhu, M. Zhu, K. Jiang and Q. Huang, *Bioorg. Chem.*, 2004, **32**, 223–233.

11 (*a*) H.-C. Becker and B. Nordén, *J. Am. Chem. Soc.*, 1997, **119**, 5798–5803; (*b*) Y. Liu, B.-H. Han, S.-X. Sun, T. Wada and Y. Inoue, *J. Org. Chem.*, 1999, **64**, 1487–1493.

12 D. Pant, H. B. Tripathi and D. D. Pant, *J. Lumin.*, 1992, **51**, 223–230.

13 Y. Liu, L. Li, H.-Y. Zhang, Z. Fan and X.-D. Guan, *Bioorg. Chem.*, 2003, **31**, 11–23.

14 (*a*) D. Neuhaus and M. Williamson, *The Nuclear Overhauser Effect in Structural and Conformational Analysis*, VCH Publishers, New York, 1989; (*b*) T. H. A. Silva, A. B. Oliveira and W. B. De Almeidab, *Bioorg. Med. Chem.*, 1997, **5**, 353–361.

15 (*a*) Y. Liu, Y.-W. Yang, H.-Y. Zhang, B.-W. Hu, F. Ding and C.-J. Li, *Chem. Biodiversity*, 2004, **1**, 481–488; (*b*) Y. Liu, G.-S. Chen, Y. Chen, F. Ding and J. Chen, *Org. Biomol. Chem.*, 2005, **3**, 2519–2523.

16 J. M. Schuette, T. Ndou, A. M. de la Peña, K. L. Greene, C. K. Williamson and I. M. Warner, *J. Phys. Chem.*, 1991, **95**, 4897–4902.

17 Y.-M. Zhang, Y. Chen, Z.-Q. Li, N. Li and Y. Liu, *Bioorg. Med. Chem.*, 2010, **18**, 1415–1420.

18 Z. Guo, Y. Jin, T. Liang, Y. Liu, Q. Xu, X. Liang and A. Lei, *J. Chromatogr., A*, 2009, **1216**, 257–263.

